Academic Journal of Science and Technology
ISSN: 2771-3032 | Vol. 14, No. 3, 2025

Automated Construction of Deep Learning Sample Sets for Impervious Surfaces Incorporating Eco-Geographic Partitions

Longchen Zhai

School of Geomatics and Urban Spatial Informatics, Beijing University of Civil Engineering and Architecture, Beijing 102600, China

Abstract: Accurate and efficient Impervious surface mapping is crucial to natural ecological protection, urban planning, land use and other fields. Currently, using deep learning methods to extract Impervious surfaces requires a large number of training samples, and visual interpretation of the samples is time-consuming and laborious. The distribution of existing labeled samples is relatively limited, which will lead to model overfitting. This paper fully considers factors such as geographical differences and efficiency, and proposes an automatic extraction technology for Impervious surfaces combined with ecological geographical zoning. Two high-precision Impervious surface products, GISA and GLC_FCS30, are fused and superimposed, and training samples are obtained through the crowd-source data OpenStreetMap mapping optimization results. A deep learning framework based on ResNeSt introduced into ASPP is used to automatically construct Impervious surface samples in different ecological geographical divisions across the country. After testing with Gaofen-1 data in the internal test areas of each partition, the overall accuracy of impermeable surface extraction exceeded 90%. The sample migration characteristic experiment shows that the model extraction accuracy within the same ecological geographical zone is the highest and the effect is significant, and the overall accuracy of models in different ecological geographical zones is increased by at least 1.44%. The method of automatically constructing Impervious surface samples proposed in this article not only achieves ideal results in terms of accuracy, but also has geographical generalization.

Keywords: Impervious water surface; Deep learning; Automatically build samples; Geographical division.

1. Introduction

In academic research, Impervious surface area (ISA) refers to natural or man-made substances that can prevent water from penetrating below the surface. It is one of the main signs of urbanization. Increases in Impervious surface can exacerbate ecological problems such as surface runoff and are critical to supporting urban environment and ecosystem management[1].

Remote sensing image data are growing rapidly in geometric progression and have become an important source of data for the extraction of surface information[2]The extraction methods of Impervious surfaces are mainly categorized into spectral mixture analysis, exponential method and machine learning algorithms. Remote sensing information extraction has gradually evolved from time-consuming manual visual interpretation to automated extraction techniques, such as machine learning and deep learning[3-5]. Training samples are the basis of deep learning model construction, and the quality and quantity of training samples decide the model classification[4]The main purpose of deep learning remote sensing image samples is to obtain samples by manual labeling and automatic acquisition. For the acquisition of deep learning remote sensing image samples, manual labeling of samples and automatic acquisition of samples are mainly used at this stage. Manual labeling refers to the visual interpretation of feature information of remote sensing images by experts, which is highly operable and accurate, but subjective and inefficient[6]. Automated sample construction methods, on the other hand, mostly use machine learning or a combination with manual interpretation, Article[7]Positive sample expansion based on supervised classification mechanism with manually labeled single positive samples to extract rural residential land in North China Plain. Article[8]Remote sensing images and corresponding historical interpretation data are used to construct a sample data set, and a deep convolutional neural network is trained to obtain a pre-trained model. The expansion of the sample library based on existing areas cannot meet the needs for rapid extraction of large-scale feature information. Kristofer Lasko[9]Fitting machine learning classifiers using spectrally balanced and randomly generated training datasets based on metric values and optimal thresholds. Article[10]The unique phenological and spectral characteristics of winter wheat are used to identify the provincial training samples of winter wheat one-class support vector machine (OCSVM). However, the classifier relies on parameter settings to achieve the same quality classification results in other areas. Therefore, constructing a sufficient and representative sample data set is crucial for deep learning to extract large-scale Impervious surfaces.[4]。

Some scholars have attempted to extract training data from historical land cover products, the[11]. Article[12]This paper discusses an automatic extraction method of land cover samples. Compared with single-source samples, automatic extraction of land cover samples using multi-source data can achieve better classification stability. Zhang et al.[13]Human comparative analysis of GLC_FCS30 in 15 experimental areas[14]、NUACI[15]、GHSL[16]、HBASE[17]Surface coverage product accuracy, experiments have proven that the overall accuracy of the GLC_FCS30 product is the highest at 95.10%[18]. Global 30-meter Impervious surface product (GISA)[19]Using the entire world as a research area to extract Impervious surfaces, the time span is as long as 37 years, and GISA's producer accuracy and user accuracy are both very high.[19]. Considering the spatiotemporal consistency and

classification stability between products, this paper proposes a method that combines optimized GISA, GLC_FCS30 surface coverage products and Gaofen-1 images to automatically construct an Impervious surface sample set.

Impervious surfaces behave similarly to bare ground in more arid areas and to bodies of water in wetter areas. Article[20]Seasonal Impervious surface extraction was carried out in Beijing and Nanjing. Vegetation, water, bare soil and surface temperature were selected as influencing factors, and geographical detectors were used to prove that precipitation has an impact on the accuracy of Impervious surface extraction. It can be seen that regional geographical factors have varying degrees of impact on Impervious surfaces. The global ecological geographical divisions (Eco-regions) established by the World Fund divide the world into 867 small ecological regions. [21]. Ecological GeographyZoning by geographic attributes, with similar biomes and regular surface cover changes, can solve the problems faced by global mapping. However, there are few studies on the automatic generation of Impervious surface samples for eco-geographic zoning. In this paper, we use the method of Impervious surface sample construction with eco-geographic zoning to automatically produce sample sets to avoid the confusion of features in different wet and dry areas.

2. Study Area and Sources

2.1. Experimental area

According to the four ecological geographical divisions divided in this article, the study area selected four representative cities nationwide, namely W-1 Urumqi City, W-2 Ili Kazakh Autonomous Prefecture, W-3 Beijing City, W-4 Wuhan City, The above cities are located in arid areas, semi-arid areas, semi-humid areas and humid areas respectively. The experimental area has a rich variety of typical land features, which is suitable for sample construction in this study. Figure 1.

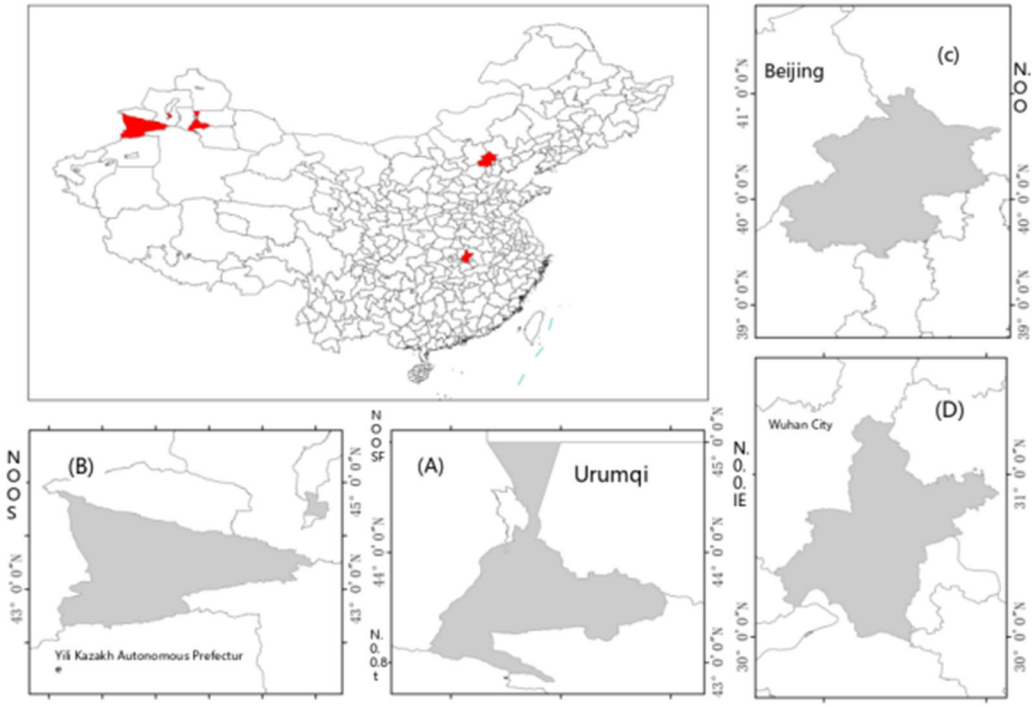

Figure 1. Schematic diagram of the experimental area (a, b, c, and d are W-1 Urumqi City, W-2 Ili Kazakh Autonomous Prefecture, W-3 Beijing City, and W-4 Wuhan City respectively)

2.2. Selection of eco-geographical zones

In order to better focus on the study of Impervious surfaces, based on the different reflectance of images of cropland, bare land, water bodies and Impervious surfaces in areas with different precipitation levels, they were divided into four major subregions based on the integration of 867 eco-geographic subregions around the globe according to the average annual precipitation, which was divided into four major subregions, as shown in Table 1[22]. The four large partitions W1, W2, W3 and W4 were finally generated. The specific ecological geographical zoning results are shown in Figure 2.

Table 1. Division of precipitation

Codenames	Average annual rainfall
W1	Arid zone <200
W2	Semi-arid area 200mm-400mm
W3	Semi-humid area 400mm-800mm
W4	Wet zone > 800

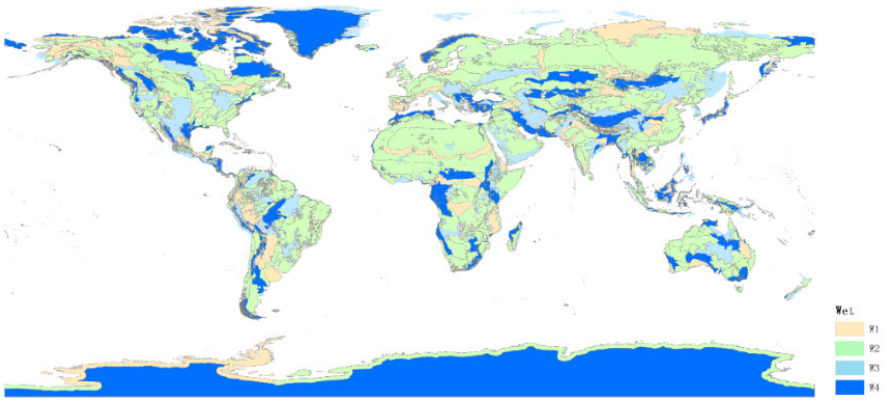

Figure 2. Geographic zoning based on precipitation

2.3. High-precision ground cover products

GLC_FCS30-2020 product and GISA product overview

Domestic and foreign researchers have released a series of global, regional or national-level 1km-30m resolution products[23]. After investigation and research on seven surface coverage products, GLC_FCS30 has better producer accuracy and verifier accuracy.[13], with more than 20 million samples, which is higher than the number of global classification samples and the user usage rate is second only to Globeland30. It contains the Impervious surface category, code-named 190; the researcher verified GISA based on the method of randomly selecting verification points, and the classification accuracy was 89 % and higher than other products and only contains impermeable and permeable surfaces[24]. Therefore, these two products were selected as the data base.

Crowd source data

The Open Street Map (OSM) project is a globally freely licensed geospatial database[25]. Cidáli[26]Integrating Globeland30 (GL30) data and the latest OSM, the updated LULC chart is better than the original GL30 in overall accuracy. This study uses OSM as an auxiliary tool for optimizing fused data to select OSM transportation facilities, buildings and other surface element types such as natural, water bodies, transportation facilities, and religious land coverage elements.[27]. The classification relationship between Impervious surfaces and these OSM surface elements is detailed in Table 2.

Table 2. Mapping relationship between OSM and classification

Classification	OSM feature categories
Impervious surfaces category	traffic transport buildings pofw
non-Impervious surface category	natural water

2.4. Formatting of auomatically construct impervious surface samples

Extracting large-scale artificial Impervious surface elements requires a large number of samples, and automatic generation of training sample sets can save time and improve efficiency. The steps of the algorithm for automatic construction of Impervious surface sample sets for eco-geographic zoning are shown in Figure 3.

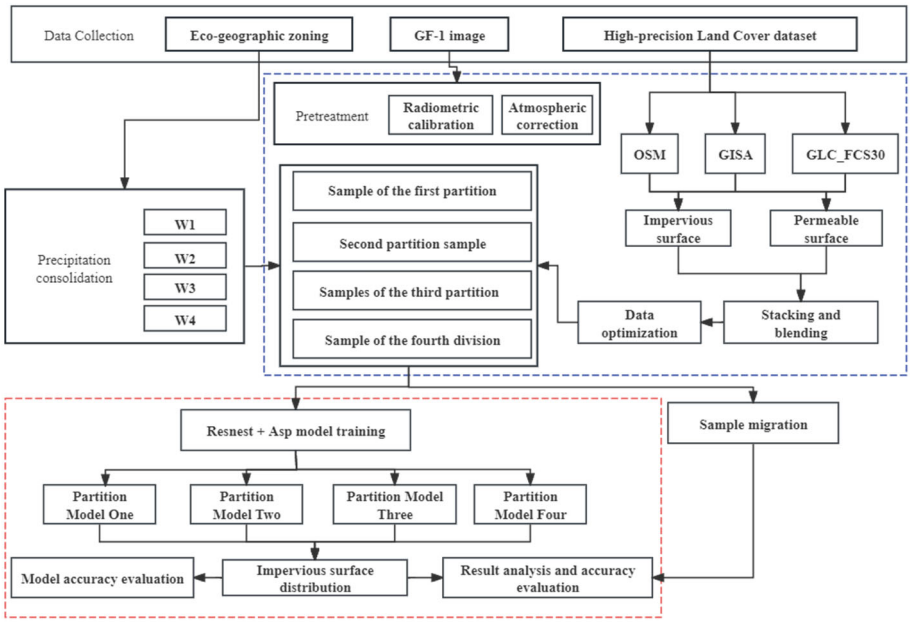

Figure 3. Production technology routes

The deep learning construction sample consists of two parts, namely the original image and label production. This article selects Gaofen-1 16m resolution image data for sample production. Taking the study area of Wuhan, China (Figure 1-d) in the humid area as an example to show the sample label production process and results in detail, the steps for other ecological geographical divisions are the same.

2.5. Data fusion

Data fusion in remote sensing is attribute fusion, which combines several complementary or repeated information according to certain rules. Label production first transforms the 2019 GISA and 2020 GLC_FCS30 products into the same coordinate system as the GF-1 image through geographical coordinate system transformation, and obtains the Impervious surfaces corresponding to the two products in Wuhan through attribute filtering and reclassification, and then combines GISA and GLC_FCS30 The Impervious surface is obtained through topological intersection. Figure 4 compares the Gaofen-1 image with the two products.

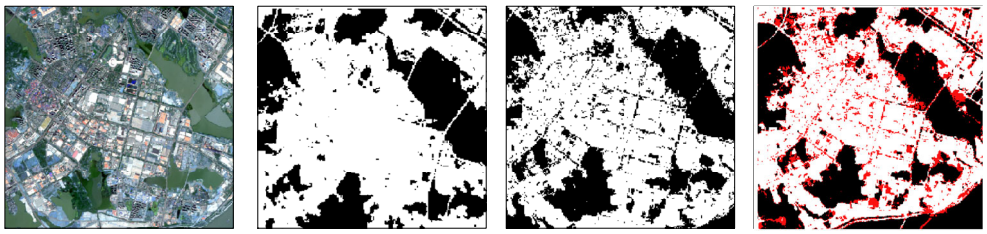

(a) (b) (c) (d)

Figure 4. Comparison of the fusion between Gaofen-1 and two products (a, b, c, and d are the original images of Gaofen-1, the GISA product, the GLC_FCS30-2020 product, and the fused product respectively; the conflict area is indicated in red and the impermeable surface Indicated in white, permeable surface in black)

2.6. Crowd-sourced data optimization

Remove the increase in Impervious surface caused by urban development in 2019-2020 and remove other categories; add the OSM Impervious surface category in 2020. Six OSM surface elements were selected and divided into two categories: permeable surface and impermeable surface according to Table 2. Subsequently, the merged features were converted to raster format and resampled to 16 meters. The conflict points in the fused data intersect with the permeable surface and impermeable surface of OSM respectively to be corrected and assigned values respectively. The final pixels that cannot be optimized by OSM are regarded as final uncertain points and assigned specific values. Taking the city of Wuhan as an example, the above process is shown in Figure 5.

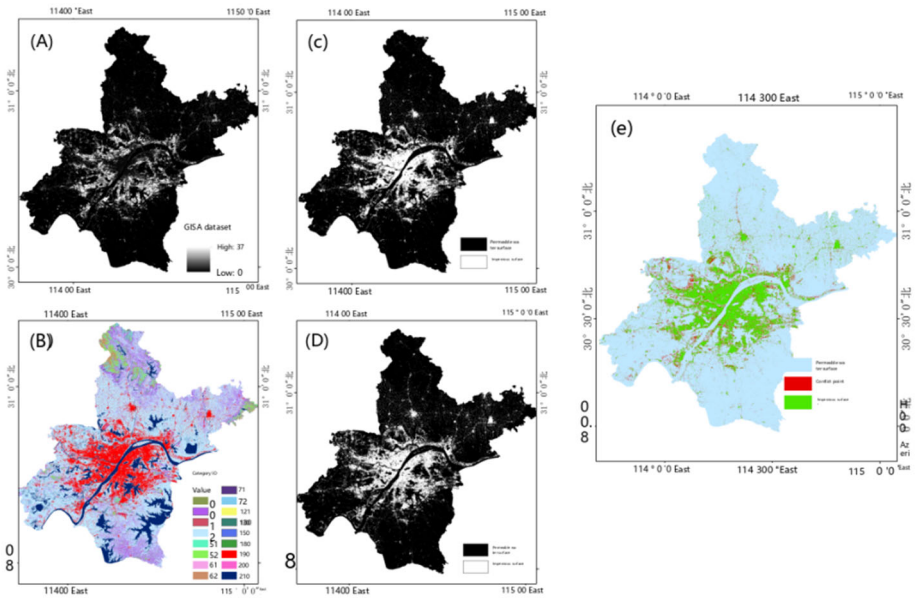

Figure 5. Wuhan classification after optimization (where a, b, c, d, and e represent Wuhan's GISA products, GLC_FCS30-2020 products, GISA product impermeable surfaces, GLC_FCS30-2020 product impermeable surfaces, and fusion optimized samples respectively)

2.7. Sample construction of eco-geographic zones

Sample construction uses GF-1 imagery, and uses the same automatic sample construction method as W-4 Wuhan City to create sample sets for W-1 Urumqi City, W-2 Ili Kazakh Autonomous Prefecture, and W-3 Beijing City for ecological geographical zoning. Model training. The samples of the four major partitions are shown in Figure 6:

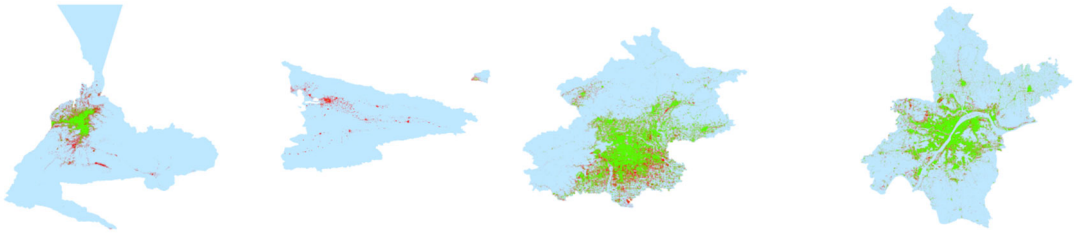

Figure 6. Results of the urban samples from the four major eco-geographical precipitation sub-regions

3. Deep Learning Models of Impervious Surfaces for Ecological Geographic Zonin

3.1. Sample preparation for eco-geographic zoning

In order to train the deep learning model, the remote sensing images of each study area are divided into small blocks of size 512 x 512. It facilitates large-scale remote sensing data processing and avoids computer memory overflow. Allowing a repetition rate of 0.1 when dividing can obtain more diverse data and improve model generalization. The images are further divided into training set, validation set and test set. The training set is used to train the developed model; the validation set is used to verify the performance of the model and adjust model parameters during the training process; the test set is used for final model evaluation after the model training is completed. When actually training the network, there are only Impervious surfaces and permeable surfaces in the labels. In order to display the labels, the pixel value 0 is changed to 255. The white color in the label map represents the impermeable surface type, and the black color represents the non-Impervious surface type. Some sample displays are shown in Figure 7.

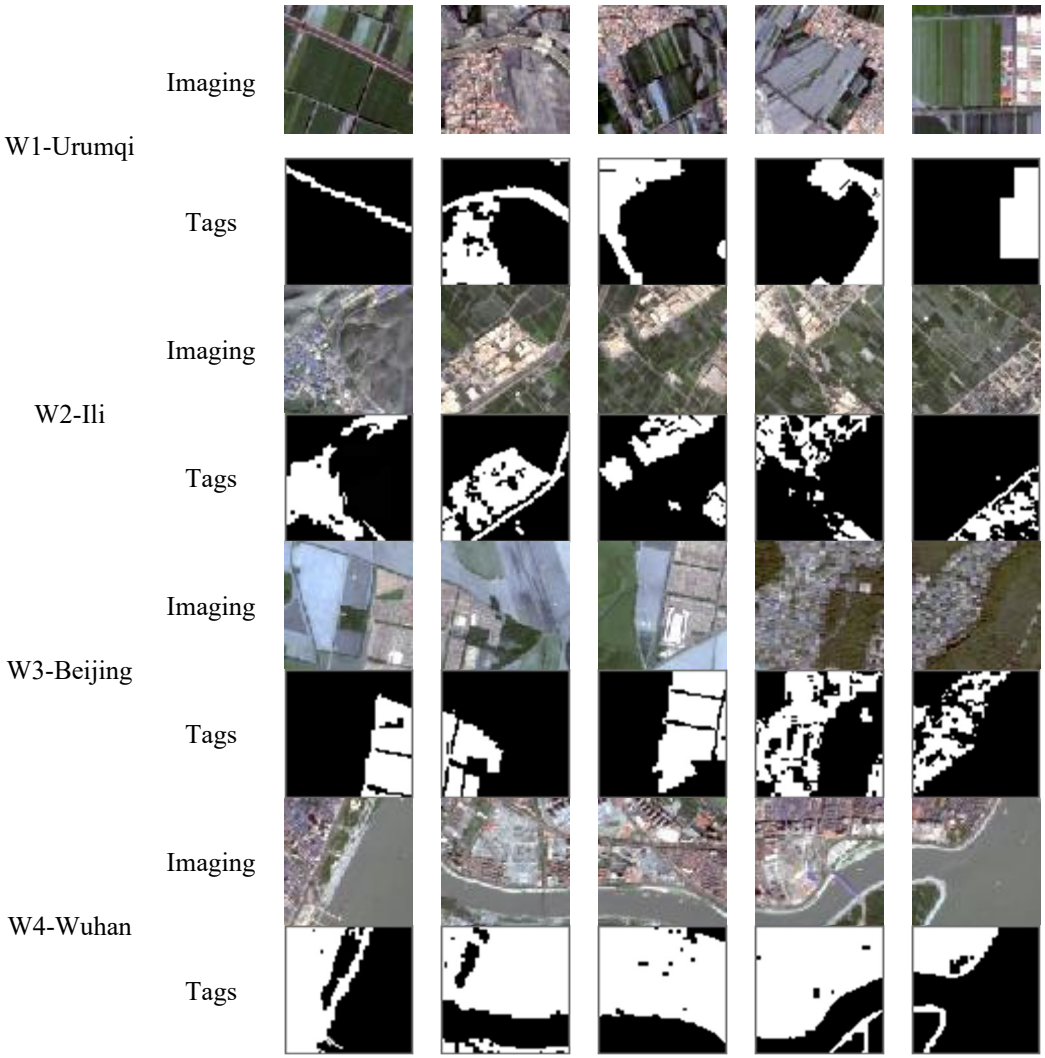

Figure 7. Display of localized samples in four partitions

3.2. Efficient Deep Learning Modeling Framework

ResNeSt (Residual Networks with Stacked Attention) is an improved general backbone network. One of its core features is that it retains the residual connection structure of ResNet and solves the gradient disappearance problem of deep networks through skip connections, allowing the network to learn more deeply and improve performance. In order to make more effective use of cross-channel information, a split-attention mechanism is introduced and an attention module is added to each residual block.

Adopt innovative grouping and segmentation strategies to extract rich channel features. First, the input images are grouped and internally segmented into multiple branches to increase capacity and capture various details and complexity. The structure consists of multiple stacked attention modules, each module has split-attention. When processing images, pay more attention to important parts of the image to improve recognition and segmentation accuracy. This study introduces the (ASPP) module to further improve network performance. The ASPP module expands the network receptive field and obtains more feature information without reducing the resolution. This design enables the network to focus more on important parts when processing Impervious and permeable surface features, improving recognition and segmentation accuracy. The network structure diagram of this study is shown in Figure 8.

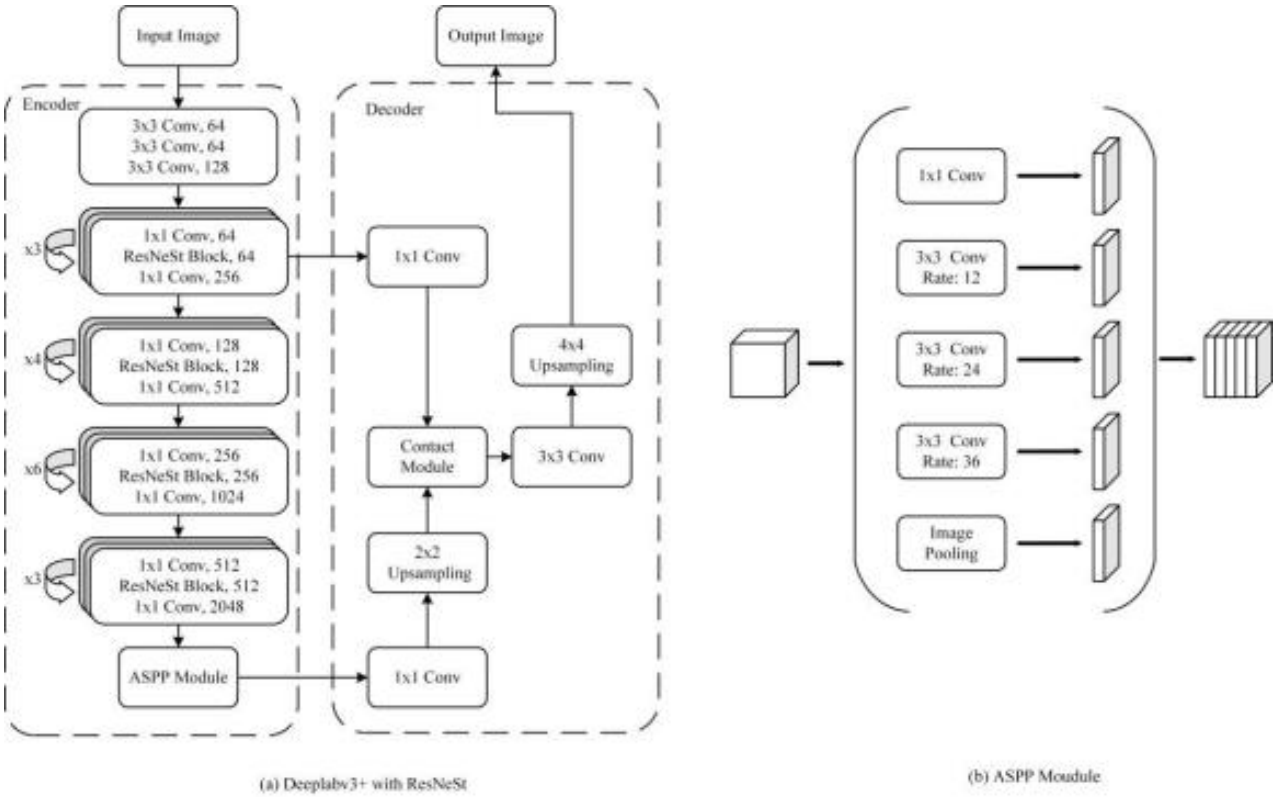

Figure 8. Diagram of the network structure of this study

First, input the image into the backbone network. After passing the first stem block, the channels are reduced to 128, and the feature dimension becomes 1/4 of the original. After the second block, the channels are reduced to 256, and the feature size is still 1/4 of the original. After the image leaves the backbone, it enters the ASPP module, uses 1x1 convolution and three atrous convolutions with expansion rates of 12, 24, and 36, obtains multi-scale information through image pooling, and uses 1x1 convolution to fuse. Then, it is merged with the first part of the second block through double upsampling and fused through 3x3 convolution. Four times upsampling is performed to obtain the original image size prediction image.

4. Experimental Results Nd Accuracy Evaluation

4.1. Automated construction of Impervious surface samples

In the second chapter of the analysis, the post-fusion conflict points are expressed as points where the two products are inconsistent in superposition. There are two main reasons: first, the GLC_FCS-2020 product is in 2020, and the GISA data is in 2019. The difference between the two products is one year, and the city The impermeable surface of development has increased; secondly, the two products use different classification systems, different source data, different mapping rules, and misclassification of products.

Finally, the conflict points of Wuhan classification pixels after OSM optimization are considered to be uncertain points. Through data comparison and image comparison before and after optimization (as shown in Figure 9 and Table 3), the situation of the impermeable surface has been significantly optimized.

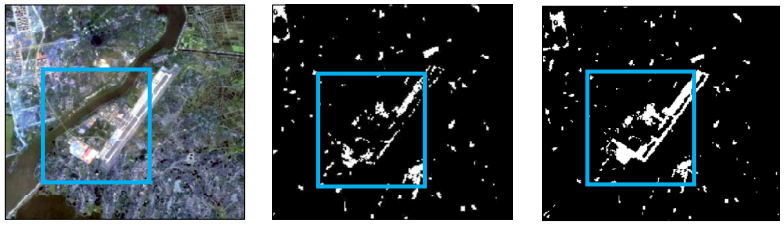

GF-1 imagery Before optimization After optimization

Figure 9. Comparison of before and after optimization

Table 3. Comparison of data before and after OSM optimization

	Impervious surface points	non-Impervious surface points	Points of conflict
Before OSM optimization	4,135,518	73,047,151	2,423,091
After OSM optimization	4,139,481	73,102,132	2,364,147

500 verification points were randomly generated at locations with consistent classification in Wuhan City for accuracy evaluation. Compare the visual interpretation of Google Earth images to verify the predicted point categories and the real point categories one by one. The data statistics of the generated confusion matrix show that there are 366 non-Impervious surface points and 134 Impervious surface points. The formula is used to calculate the overall consistent classification of Impervious surfaces and non-Impervious surfaces in Wuhan obtained by this research method. The accuracy is 99.2%, and the points that are still wrong after optimization are mainly the wrong markings of green belts in urban areas.

4.2. ResNeSt model testing

In order to investigate the deep learning model performance in different eco-geographic subzones. Four major test areas with a raster size of 6897 × 6897 were randomly selected for model testing in the above four major precipitation subzones, respectively.

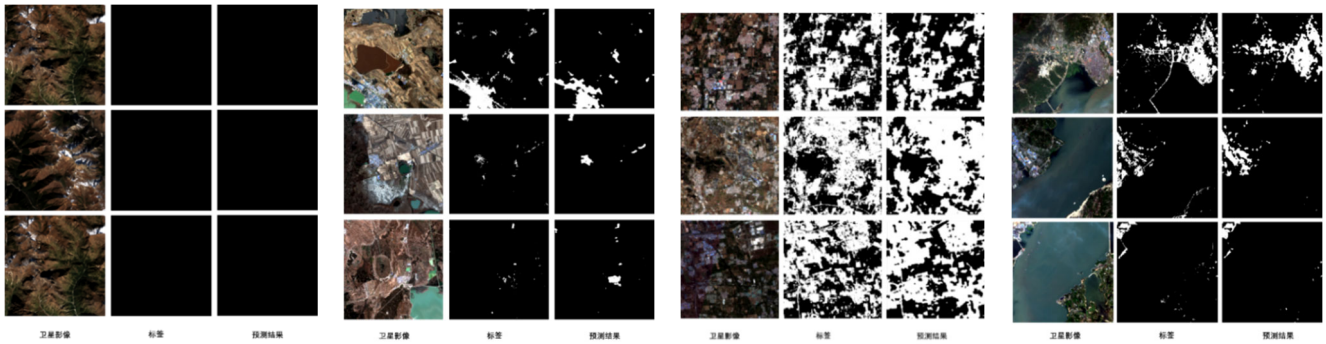

W1 (arid area) W2 (semi-arid area) W3 (semi-humid area) W4 (wet zone)

Figure 10. W1 Comparison of W2, W3, W4 images, tags and prediction results

In order to verify the feasibility of the algorithm, six key evaluation indicators: Intersection over Union, IoU), Accuracy, Acc), Dice coefficient Fscore, Precision and recall rate evaluate the deep learning semantic segmentation model. Each of these indicators has its own focus, reflecting the performance of the model.

The formulae for these indicators are as follows.

$$\mathrm{mIoU} = \frac{\mathrm{TP}}{\mathrm{TP+FP+FN}} \tag{1}$$

$$\mathrm{mAcc} = \frac{\mathrm{TP+TN}}{\mathrm{TP+TN+FP+FN}} \tag{2}$$

$$\mathrm{mDice} = \frac{2\cdot\mathrm{TP}}{2\cdot\mathrm{TP+FP+FN}} \tag{3}$$

$$\mathrm{mFscore} = \frac{2\cdot\mathrm{Precision}\cdot\mathrm{Recall}}{\mathrm{Precision+Recall}} \tag{4}$$

$$\mathrm{mPrecision} = \frac{\mathrm{TP}}{\mathrm{TP+FP}} \tag{5}$$

$$\mathrm{mRecall} = \frac{\mathrm{TP}}{\mathrm{TP+FN}} \tag{6}$$

TP: Number of correctly recognized pixels, FP: Number of pixels incorrectly identified, TN (True Negative): number of correct unrecognized pixels, FN: Wrong number of unrecognized pixels.

Tested by the data of Gaofen No.1 in the experimental area, The overall accuracy rate (aAcc) of the model in the verification of W1-W4 test area is more than 92%, among which there are fewer Impervious surfaces in arid areas, so it shows perfect data,as shown in table 4. The average intersection union ratio (mIoU) and the average accuracy rate (mAcc) both exceeded 76% and 82%, showing the excellent performance of the deep learning model.

Table 4. Model Accuracy of W1-W4 Area

Area	aAcc	mIoU	mAcc	mDice	mFscore	mPrecision	mRecall
W1	1	1	1	1	1	1	1
W2	0.996	0.7685	0.8221	0.8501	0.8501	0.8835	0.8221
W3	0.9266	0.791	0.8799	0.8781	0.8781	0.8763	0.8799
W4	0.9902	0.7953	0.8584	0.8727	0.8727	0.8883	0.8584

4.3. Sample migration experiments for eco-geographical subdivisions

In order to verify the effectiveness of constructing samples combined with ecological geographical division, migration experiments were designed. Jiangxi Province, located in the W4 humid area, is selected as the migration experimental area, which is located in the southeast of China and on the south bank of the middle and lower reaches of the Yangtze River. Due to the large geographical area, this paper cuts a relatively balanced regional GF-1 image for migration experiment in Jiangxi, as shown in Figure 11.

Figure 11. Jiangxi experimental region

The four major eco geographical zoning models were used to predict the Jiangxi experimental area located in W4, and the extraction accuracy of Impervious surface under different eco geographical zoning models was compared. In Jiangxi experimental area, 100 verification points were randomly selected for visual interpretation. Jiangxi has slightly different classification results in the ResNeSt network trained with the same number, proportion and basic parameters in four divisions, and has achieved good classification results. The specific overall accuracy and Kappa are shown in Table 5. The extraction accuracy in the model of W4 Wuhan sample training in the same humid area reaches 85.52%

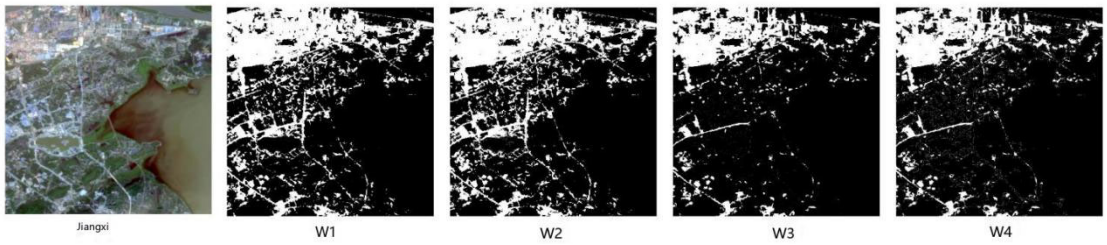

Figure 12. Comparison of experimental results of

Table 5. Precision index of sample migration classification results of ecological geographical division based on ResNeSt

	W1-Urumqi	W2-Ili	W3-Beijing	W4-Wuhan
Overall accuracy in Jiangxi (%)	83.23	83.52	84.08	85.52
Jiangxi kappa	0.72	0.72	0.74	0.76

The white part of the experimental results represents the impermeable water class, and the black part represents other classes. According to the above classification results of Impervious surface, the sample set generated by the automatic sample construction method in this paper is better for extracting Impervious surface for depth learning, and the contour is more complete and clear. In Jiangxi classification, W3 and W4 sample sets distinguish bare land better than W1 W2 sample set training model. W1 and W2 mistakenly divide the bare ground with high reflectivity into impermeable water surfaces. The advantages of automatic sample construction combined with eco geographical zoning are verified.

5. Conclusion

In this paper, the method of developing artificial Impervious surface product set combined with ecological geographical division is proposed, and the permeable surface and Impervious surface sample database are automatically constructed. Integrate high-precision surface coverage products, and optimize the deep learning sample set using multiple source data. The difference and accuracy of different product classification systems were analyzed. Through the data test of Gaofen No. 1 in the experimental area, the overall accuracy rate (aAcc) of the model in the validation of the four zones was more than 92%, and the average intersection/merge ratio (mIoU) and average accuracy rate (mAcc) were more than 76% and 82%, showing the excellent ability to correctly classify various categories. For the first time, the knowledge of eco geographical precipitation zoning was used to construct Impervious surface sample set. Based on the law of surface change and the characteristics that Impervious surface is easily confused in different precipitation regions, it provides ideas for large-scale sample production.

In this paper, we propose a method for the production of global ten-meter Impervious surface products, which provides a basis for deep learning image classification. However, the method in this paper is used for the extraction and validation of Impervious surface samples with a single sample type, which needs to be improved. The automatic construction method is also applicable to other feature classifications, such as water bodies, cultivated land, forest land, and so on.

References

[1] Tang Y , Shao Z , Huang X , et al. Mapping Impervious Surface Areas Using Time-Series Nighttime Light and MODIS Imagery[J]. Remote Sensing, 2021, 13(10).

[2] Feng Quan-Taki,Chen Po-an,Li G.Q. et al.2022.A review of research on sample datasets of remote sensing images. Journal of Remote Sensing,26(4):589-605

[3] He Ying. Application of office information extraction based on remote sensing technology in the third land survey [D]. Jilin University, 2019

[4] Building Qin. Application of Impervious surface extraction and space-time evolution analysis based on deep learning [D]. Zhejiang University, 2021. DOI: 10.27461/d.cnki.gzjdx.2021.002808

[5] Lv X, Shao Z, Ming D, et al. Improved object-based convolutional neural network (IOCNN) to classify very high-resolution remote sensing images[J]. International Journal of Remote Sensing, 2021, 42(21): 8318-8344.

[6] Pang Bo, Huang Zuoji, Wu Yanlan, etc. Extraction and mapping of Impervious surface from high resolution remote sensing image based on improved full convolution neural network [J]. Remote Sensing Information, 2020,35 (04): 47-55

[7] Lu Chen, Yang Xiaomei, Wang Zhihua. Remote sensing extraction method of block type rural residential areas based on automatic sample expansion [J]. Journal of Geoinformation Science, 2018,20 (09): 1306-1315

[8] Li Xin, Yang Yi, Wang Ning, etc. Automatic generation of remote sensing image samples and intelligent iterative classification method [J]. Surveying and Mapping Science, 2022,47 (08): 197-203. DOI: 10.16251/j.cnki.1009-2307.2022.08.022

[9] Lasko, K.; Maloney, M.C.; Becker, S.J.; Griffin, A.W.H.; Lyon, S.L.; Griffin, S.P. Automated Training Data Generation from Spectral Indexes for Mapping Surface Water Extent with Sentinel-2 Satellite Imagery at 10 m and 20 m Resolutions. Remote Sens. 2021, 13, 4531. https://doi.org/10.3390/rs13224531

[10] Yang G, Yu W, Yao X,et al.AGTOC: A novel approach to winter wheat mapping by automatic generation of training samples and one-class classification on Google Earth Engine - ScienceDirect[J].International Journal of Applied Earth Observation and Geoinformation, 102[2024-04-10].DOI:10.1016/j.jag.2021.102446.

[11] Radoux, J., Lamarche, C., Van Bogaert, E: Automated training sample extraction for global land cover mapping, Remote Sens., 6, 3965–3987.

[12] Zhang, X. and Liu, L.: Development of a global 30 m Impervious surface map using multi-source and multi-temporal remote sensing datasets with the Google Earth Engine platform, Zenodo.

[13] Zhang, X., Liu, L., Chen, X.: Fine LandCover Mapping in China Using Landsat Datacube and an Operational SPECLib-Based Approach, Remote Sens., 11, 1056.

[14] Gong Peng, Wang Jie, Yu Le, et al. Finer resolution observation and monitoring of global land cover: first mapping results with Landsat TM and ETM+ data [J]. International Journal of Remote Sensing, 2013, 34(7): 2607-2654.

[15] Liu Xiaoping, Hu Guohua, Chen Yimin, et al. High-resolution multi-temporal mapping of global urban land using Landsat images based on the Google Earth Engine Platform [J]. Remote Sensing of Environment, 2018, 209:227-239.

[16] Pesaresi Martino, Syrris Vasileios, Julea Andreea. A New Method for Earth Observation Data Analytics Based on Symbolic Machine Learning [J]. Remote Sensing, 2016, 8(5):399.

[17] Wang P., Huang C., Brown de Colstoun E. C., et al. Global Human Built-up And Settlement Extent (HBASE) Dataset From Landsat [M]. Palisades, NY: NASA Socioeconomic Data and Applications Center (SEDAC). 2017:1-11.

[18] Zhu Ling, Jia Tao, Shi Ruming. Update and integration of global surface coverage products [M]. Science Press, 2020

[19] Huang X, Jiayi L I, Yang J, et al. 30m global immediate surface area dynamics and urban expansion pattern observed by Landsat satellites: From 1972 to 2019 [J]. Science of China: Earth Sciences, 2021,64 (11): 12. (GISA)

[20] Hou Xingxing, Zhang Xinchang, Zhao Yi, et al. Research on Deep Learning to Extract Natural Environmental Impact Factors of Impervious Water Surface [J]. Surveying and Mapping Science, 2022,47 (11): 73-84. DOI: 10.16251/j.cnki.1009-2307.2022.11.010

[21] Olson., D.M.., Dinerstein., E.: Terrestrial ecoregions of the world: a new map of life on Earth. Bioscience 51(11):933-938.

[22] Chen Xu. Construction and Application of Knowledge Base for Global Eco geographical Zoning [D]. Beijing Jianzhu University, 2017

[23] Zhang X , Liu L , Wu C ,et al.Development of a global 30 m Impervious surface map using multisource and multitemporal remote sensing datasets with the Google Earth Engine platform[J].Earth System Science Data, 2020, 12(3):1625-1648.DOI:10.5194/essd-12-1625-2020.

[24] Chen Guandong. Research on urban Impervious layer extraction method based on multi-source remote sensing image fusion [D]. Beijing University of Technology, 2018

[25] OpenStreetMap in GIScience; Jokar Arsanjani, J., Zipf, A., Mooney, P., Helbich, M., Eds.; Lecture Notes in Geoinformation and Cartography; Springer: Cham, Switzerland, 2015.

[26] Cidália, Costa, Fontesup, et al. Generating Up to Date and Detailed Land Use and Land Cover Maps Using OpenStreetMap and GlobeLand30[J]. International Journal of Geo-Information, 2017, 4(6).

[27] Fonte C , Minghini M , Antoniou V , et al. An automated methodology for converting OSM data into a land use/cover map[C]// 6th International Conference on Cartography and GIS. 2016.